

Journal Watch

IEEE Transactions on Wireless Communications, March, 2019

Sai Subramanyam Thoota
SPC Lab, Department of ECE
Indian Institute of Science

March 16, 2019

Efficient Beam Alignment for Millimeter Wave Single-Carrier Systems with Hybrid MIMO Transceivers

Goal

- To design a suitable signaling between the BS and the UE, find an estimate of the AoA-AoD power spread function (PSF), and identify an AoD-AoA pair with a sufficiently large strength

Contributions

- A novel efficient BA scheme for single-carrier mmwave communications with hybrid digital analog (HDA) transceivers and frequency selective multipath channels
 - Time domain signaling scheme, and PN sequences with good correlation properties used
- Designed for general and realistic mmwave channel model
 - Fast time variations due to Doppler, frequency selectivity and AoA-AoD sparsity
- Impact of the PN sequence length due to Doppler
- System-level scalability and Low-complexity beam direction estimation
 - Identification of the strongly coupled AoD-AoA pairs as a non-negative least squares problem
 - No hierarchical UL-DL beam training

Channel Model:

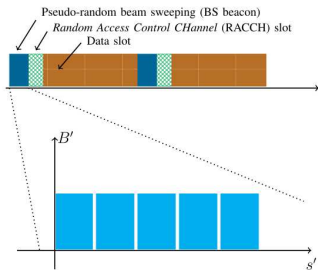
- Sparse collection of multipath components in the continuous AoD-AoA-delay (ϕ, θ, τ) domain, including LoS and NLoS paths
- WSSUS model assumed

Power spread function (PSF):

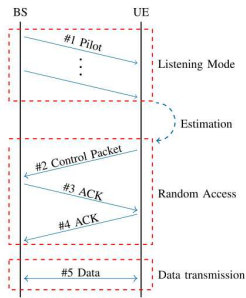
- Average signal energy distribution over the AoD-AoA-delay domain is described by the PSF $f_p(\phi, \theta, \tau)$
- Locally time invariant as long as the propagation geometry does not change significantly
- Only few discrete delays in practical channel measurements
- Unknown

BA Problem:

- Design a suitable signaling between the BS and the UE, find an estimate of the AoA-AoD PSF, and identify an AoA-AoD pair (ϕ_0, θ_0) with a sufficiently large strength $f_p(\phi_0, \theta_0)$
- Pseudo-random sequences as the probing signals
- Formulate the PSF estimation as the LS solution of an underdetermined system of linear equations, and solve using NNLS approach



(a)



(b)

Fig. 2. (a) (Top) Frame structure of the proposed Beam Alignment (BA) scheme. (Bottom) Each beacon slot consists of S PN sequences indexed by $s' \in [S]$, and all the PN sequences have access to the whole effective bandwidth $B' \leq B$. (b) Illustration of the proposed BA process between the BS and a generic UE, where the procedures (#2~#5) are independently done at each UE, and all the UEs share the same BS beamforming codebook (#1).

- Equivalent channel after BA can be represented by a SISO channel
- Single tap, frequency flat
- Beamspace representation of the channel
 - Each tap is sparse in the beamspace domain

BS Channel Probing and UE Sensing

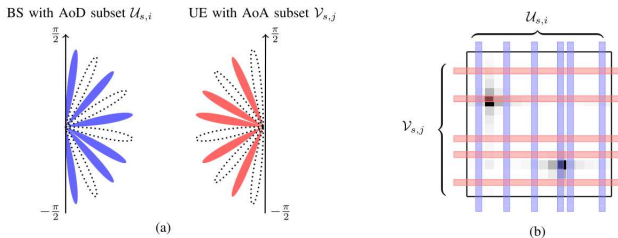


Fig. 3. (a) Illustration of the subset of AoA-AoDs at time slot s probed by the i -th beacon stream transmitted by the BS and received by the j -th RF chain of the UE, for $M = N = 10$. The AoD subset is given by $\mathcal{U}_{s,i} = \{1, 3, 4, 6, 8, 10\}$ (numbered counterclockwise) with beamforming vector $\check{\mathbf{u}}_{s,i} = \frac{1}{\sqrt{6}}[1, 0, 1, 0, 1, 0, 1, 1, 0, 1]^T$. The AoA subset is given by $\mathcal{V}_{s,j} = \{2, 4, 5, 7, 9\}$ (numbered counterclockwise) with receive beamforming vector $\check{\mathbf{v}}_{s,j} = \frac{1}{\sqrt{5}}[0, 1, 0, 1, 1, 0, 1, 0, 1, 0]^T$. (b) The channel gain matrix $\hat{\Gamma}$ (with two strong MPCs indicated by the dark spots) measuring along $\mathcal{V}_{s,j} \times \mathcal{U}_{s,i}$.

Received beacon signal at the UE:

$$\begin{aligned}
 y_{s,i,j}[k] &= \sum_{l=1}^L \sqrt{E_{\text{dim}}} \check{\mathbf{v}}_{s,j}^H \check{\mathbf{H}}_{s,l} \check{\mathbf{u}}_{s,i} R_{i,i}^l(kT_c - \tau_l) + z_{s,j}^c[k] \\
 &= (\check{\mathbf{u}}_{s,i} \otimes \check{\mathbf{v}}_{s,j}^*)^T \check{\mathbf{H}}_s \mathbf{c}_k^i + z_{s,j}^c[k] \\
 &= \mathbf{g}_{s,i,j}^T \check{\mathbf{H}}_s \mathbf{c}_k^i + z_{s,j}^c[k]
 \end{aligned}$$

- Quadratic non-coherent detection
 - Energy at the output of the matched filter accumulated to get the quadratic measurements
- After T beacon slots, the UE obtains a total number of $M_{RF} N_{RF} T$ equations given by

$$\mathbf{q} = \mathbf{B} \cdot \text{vec}(\mathbf{\Gamma}) + \check{N}_c N_0 R^x(0) \cdot \mathbf{1} + \tilde{\mathbf{w}}$$

- NNLS problem solved using standard optimization techniques

$$\mathbf{\Gamma}^* = \arg \min_{\mathbf{\Gamma} \in \mathbb{R}_+^{N \times M}} \|\mathbf{B} \cdot \text{vec}(\mathbf{\Gamma}) + \check{N}_c N_0 R^x(0) \cdot \mathbf{1} - \mathbf{q}\|^2$$

Linear Precoding With Low-Resolution DACs for Massive MU-MIMO-OFDM Downlink

Goal

- To characterize the uncoded/coded BER and achievable sum rate of a massive MU-MIMO-OFDM downlink (DL) system with finite-resolution DACs and linear precoding

Contributions

- Lower bound on the information theoretic sum rate achievable with linear precoding and oversampling finite resolution DACs using Busgang's theorem
- Approximate model for the distortion caused by the DACs, which takes into account the inherent spatial and temporal correlation in the DAC distortion
 - Accurate approximation of the signal-to-interference-noise-distortion (SINDR) ratio
 - To derive an approximation of the uncoded BER achievable with QPSK
- Simpler approximation for the DAC distortion, which treats noise as white
 - Accurate for medium to high resolution DACs, and when the OSR is not too high

System Model

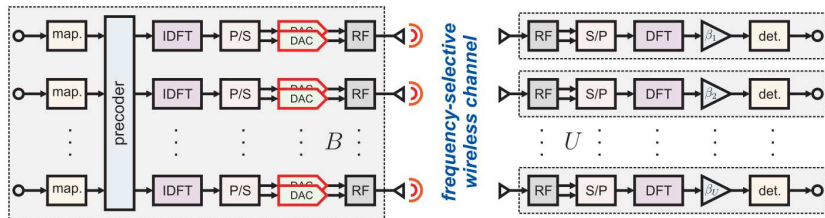


Fig. 1. Overview of the massive MU-MIMO-OFDM downlink with low-resolution DACs at the BS. Left: A B antenna BS performs linear precoding and generates the per-antenna OFDM time-domain signals that are passed through low-resolution DACs (highlighted with red color). Right: U single-antenna UEs perform independently OFDM demodulation and data detection. In the figure, “map.” and “det.” stand for mapper and detector, respectively.

- Oversampling DACs: Number of subcarriers N greater than the number of subcarriers designated for data (S)
- Oversampling rate (OSR) $\xi = N/S$
- DAC is modeled as a uniform quantizer
- MRT and ZF precoding considered
- Transmitted vector:

$$\mathbf{x}_n = \mathcal{Q}(\mathbf{z}_n)$$

- Frequency domain received signal in vectorized form

$$\text{Without quantization : } \hat{\mathbf{y}} = \hat{\mathbf{H}}\hat{\mathbf{x}} + \hat{\mathbf{w}}$$

$$\begin{aligned} \text{With quantization : } \hat{\mathbf{y}} &= \hat{\mathbf{H}} (\mathbf{F}_N \otimes \mathbf{I}_B) \mathbf{x} + \hat{\mathbf{w}} \\ &= \hat{\mathbf{H}} (\mathbf{F}_N \otimes \mathbf{I}_B) \mathcal{Q} \left((\mathbf{F}_N^H \otimes \mathbf{I}_B) \hat{\mathbf{P}}\mathbf{s} \right) + \hat{\mathbf{w}}. \end{aligned} \quad (17)$$

- Bussgang's Theorem: For Gaussian inputs, $\mathcal{Q}(\mathbf{z})$ can be decomposed into two components: a linear function in \mathbf{z} , and a distortion that is uncorrelated with \mathbf{z}

$$\mathbf{x} = \mathcal{Q}(\mathbf{z}) = \mathbf{G}\mathbf{z} + \mathbf{d}$$

- Achievable sum-rate analysis with Gaussian inputs (Lower bound derivation)
- SINDR:

$$\gamma_{u,k}(\hat{\mathbf{H}}) = \frac{\left[|\hat{\mathbf{H}}_k \text{diag}(\mathbf{g}) \hat{\mathbf{P}}_k|^2 \right]_{u,u}}{\sum_{v \neq u} \left[|\hat{\mathbf{H}}_k \text{diag}(\mathbf{g}) \hat{\mathbf{P}}_k|^2 \right]_{u,v} + D_{u,k}(\hat{\mathbf{H}}) + N_0}$$

where

$$\begin{aligned} D_{u,k}(\hat{\mathbf{H}}) &= \left[\hat{\mathbf{H}} (\mathbf{F}_N \otimes \mathbf{I}_B) \mathbf{C}_d (\mathbf{F}_N^H \otimes \mathbf{I}_B) \hat{\mathbf{H}}^H \right]_{u+kU, u+kU} \end{aligned}$$

Exact and Approximate Distortion Models to compute \mathbf{C}_d

$$\mathbf{C}_z = (\mathbf{F}_N^H \otimes \mathbf{I}_B) \widehat{\mathbf{P}} \widehat{\mathbf{P}}^H (\mathbf{F}_N \otimes \mathbf{I}_B).$$

$$\mathbf{C}_d = \mathbb{E} [\mathbf{d}\mathbf{d}^H] = \mathbf{C}_x - \mathbf{G}\mathbf{C}_z\mathbf{G}.$$

Computation of \mathbf{C}_x

- For the 1-bit DAC case, arcsine law is used

$$\mathbf{C}_x = \frac{2P}{\pi\xi B} \left(\arcsin \left(\text{diag}(\mathbf{C}_z)^{-\frac{1}{2}} \Re\{\mathbf{C}_z\} \text{diag}(\mathbf{C}_z)^{-\frac{1}{2}} \right) \right. \\ \left. + j \arcsin \left(\text{diag}(\mathbf{C}_z)^{-\frac{1}{2}} \Im\{\mathbf{C}_z\} \text{diag}(\mathbf{C}_z)^{-\frac{1}{2}} \right) \right).$$

- For multibit DAC, numerical integration needs to be done which is time consuming
 - Rounding approximation: The error vector approximated using a rounding function
 - Diagonal approximation: Quantization distortion modeled as a white process (off diagonal elements are zeros)

Joint Transmit and Circuit Power Minimization in Massive MIMO With Downlink SINR Constraints: When to Turn on Massive MIMO?

Goal

- To find the optimal number of base station (BS) antennas and transmission powers that minimize the power consumption while satisfying each user's effective signal-to-interference-and-noise-ratio constraint and the BSs' power constraints

Contributions

- The number of BS antennas and transmission powers jointly optimized, while satisfying individual power and SINR constraints for both single cell and multicell setups
- Closed form expressions for the optimum number of antennas and transmission powers when using MRT or ZF precoding for a single cell system
- Reformulate the joint optimization problem as a geometric programming problem for a multicell case and solve it

System Model

- Multiple cells with multiple antennas, single antenna UEs, TDD mode of operation
- Uplink (orthogonal) pilot transmission followed by downlink data transmission

Single cell System

- MMSE channel estimation
- MRT and ZF precoding

$$\begin{aligned} & \underset{\mathbf{p} \succeq 0, \bar{M} \in \mathbb{Z}^+}{\text{minimize}} && \sum_{k=1}^K p_k \\ & \text{subject to} && \text{SINR}_k \geq \alpha_k, \\ & && \bar{M} \leq \bar{M}_{\max}, \\ & && \sum_{k=1}^K p_k \leq \rho_d, \end{aligned} \tag{P1}$$

- Results on the feasibility of the problem
 - Optimal solution occurs when $\bar{M} = \bar{M}_{\max}$
 - As the number of antennas increases, the total transmission power will decrease
- Closed form solution

- Circuit power also considered in the cost function

$$\begin{aligned}
 & \underset{\mathbf{p} \succeq 0, \bar{M} \in \mathbb{Z}^+}{\text{minimize}} && c\bar{M} + \sum_{k=1}^K p_k \\
 & \text{subject to} && \text{SINR}_k \geq \alpha_k, \\
 & && \bar{M} \leq \bar{M}_{\max}, \\
 & && \sum_{k=1}^K p_k \leq \rho_d.
 \end{aligned} \tag{P2}$$

- Relation between the optimum number of antennas for MRT and ZF
- (P3) and (P4) problems solved in the context of multi cell system and the optimal number of antennas and the transmission powers
 - Closed form solution for P3
 - P4 solved using a geometric program approach

Hybrid Precoder Design for Cache-Enabled Millimeter-Wave Radio Access Networks

Goal

- Design of a hybrid precoder for the delivery phase of downlink cache-enabled mmwave radio access networks (CeMm-RANs)
- Maximization of the minimum user rate under a fronthaul capacity constraint, eRRH transmit power constraint, and a constant modulus constraint on the analog precoder
- Hard fronthaul information transfer (HFIT): hard information of the requested uncached files sent to the eRRHs via the fronthaul links
- Soft fronthaul information transfer (SFIT): quantized version of the precoded signals of the requested uncached files sent to the eRRHs via the fronthaul links

Contributions

- Joint optimization of the analog and digital precoders employing HFIT and SFIT
- Two algorithms developed
 - Successive approximation method to convexify the non convex objective function to design the digital precoder
 - Taylor series expansion to optimize the phases of the analog precoder
- Numerical experiments and performance study

Other Interesting Papers

- 1 Multi-Agent Reinforcement Learning for Efficient Content Caching in Mobile D2D Networks
- 2 Scheduling for VoLTE: Resource Allocation Optimization and Low-Complexity Algorithms
- 3 Periodic Analog Channel Estimation Aided Beamforming for Massive MIMO Systems
- 4 Stochastic Geometry-Based Uplink Analysis of Massive MIMO Systems With Fractional Pilot Reuse
- 5 Compensation of Phase Noise in Uplink Massive MIMO OFDM Systems
- 6 Activity Detection for Massive Connectivity Under Frequency Offsets via First-Order Algorithms
- 7 Average Age of Information With Hybrid ARQ Under a Resource Constraint
- 8 Liquid State Machine Learning for Resource and Cache Management in LTE-U Unmanned Aerial Vehicle (UAV) Networks